Response of toroidal drift modes to profile evolution: a small-ELM model?

A. Bokshi[1], D. Dickinson[1], C. M. Roach[2], H. R. Wilson[1]

[1] *York Plasma Institute, Dept. of Physics, University of York, Heslington, York, YO10 5DD, UK*

[2] *CCFE Fusion Association, Culham Science Centre, Abingdon, Oxon, OX14 3DB, UK*

Introduction

Toroidal drift instabilities are characterised by short wavelengths perpendicular to the magnetic field line and extended structure along it. And as a result of their radial localisation, these instabilities experience a weak radial equilibrium variation. The ballooning theory exploits this scale separation. To the lowest order in toroidal mode number n, the formalism provides the mode structure along the field line and local complex eigenvalue $\Omega_0(x) = \omega_0(x) + \mathrm{i}\gamma_0(x)$ (x is a radial variable). To construct the full global mode structure and global (true) complex mode frequency $\Omega = \omega + \mathrm{i}\gamma$ from the leading order local results, we need to proceed to the next order in n. This higher-order theory then predicts two types of global mode structures depending on the equilibrium profiles for all toroidal microinstabilities [1, 2]: the *Isolated Mode* (IM) and the *General Mode* (GM). The IM exists for the special situation when the maxima in $\omega_0(x)$ and $\gamma_0(x)$ are co-located. This mode will typically balloon at the outboard midplane and have a strong global growth. The GM, however, does not have any constraint on $\Omega_0(x)$ and is therefore always accessible. It will peak at the top/bottom of the poloidal plane[1] and is much more stable.

Model system

We demonstrate the essential physics with a global electrostatic toroidal fluid-ITG model for the perturbed potential $\phi_1(x,\theta)$ in a circular cross-section geometry with adiabatic electrons [3]:

$$\left[\rho_s^2\frac{\partial^2}{\partial x^2} - k_\theta^2\rho_s^2 - \frac{\sigma^2}{\Omega^2}\left(\frac{\partial}{\partial\theta} + \mathrm{i}nq'x\right)^2 - \frac{2\varepsilon_n}{\Omega}\left(\cos\theta + \mathrm{i}\frac{\sin\theta}{k_\theta}\frac{\partial}{\partial x}\right) - \frac{\Omega-1}{\Omega+\eta_s}\right]\phi_1(x,\theta) = 0. \tag{1}$$

The equilibrium parameters are defined in reference [3] (though note that Ω is normalised to the electron diamagnetic frequency ω_{*e}). The parameters used in our simulations have been defined in table 1 and are broadly comparable to those found in the pedestal.

Table 1: *Equilibrium parameters used in simulations.*

a	$k_\theta\rho_i$	$\hat{s}$	ε_n	τ	q	n	m_0	$\gamma_E = \mathrm{d}\Omega_\phi/\mathrm{d}q$
0.5	0.2	25.0	0.08	1.0	1.4	50	70	[-0.7, 0.7]

[1] In general, the poloidal location where the IM/GM peaks would depend on profiles, shaping etc.

Eqn. 1 is solved by decomposing $\phi_1(x,\theta)$ into poloidal harmonics, i.e. $\phi_1(x,\theta) = \sum_m \phi_m(x)\exp(im\theta)$, and mapping the complex frequency $\Omega_m \to i\partial/\partial t$ for each ϕ_m. Toroidal flow-shear Ω'_ϕ is included through a Doppler-shift, i.e. $\Omega \to \Omega + n\Omega'_\phi x$. An instantaneous complex mode frequency $\Omega_m(t) = i\partial \ln \phi_m/\partial t$ is evaluated at the rational surfaces where the poloidal modes m are expected to peak. For an eigenmode, we expect $\Omega_m(t) = \Omega$ for all m and independent of time.

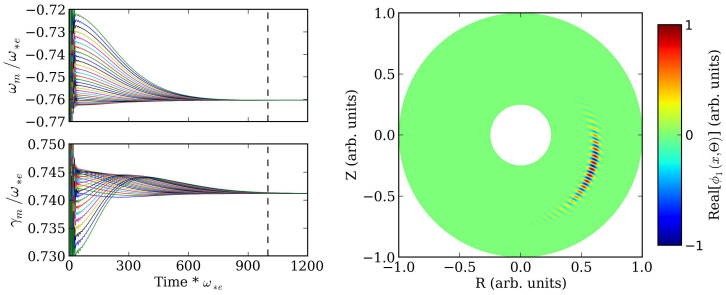

Figure 1: *(Left) Evolution of $\Omega_m(t)$. The instability is an eigenmode when $\Omega_m(t) \to \Omega$ (vertical line). (Right) The corresponding eigenfunction.*

Stationary plasma profiles

Simulations in this section were performed using the new initial-value code, holding all plasma profiles fixed in time. The simulations were initialised with noise, and after sufficient time, the solution converges to an eigenmode (Fig. 1).

Effect of flow-shear

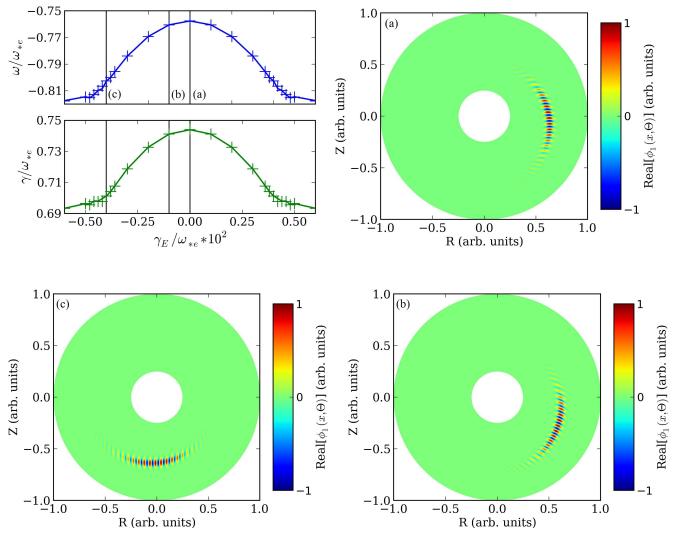

Figure 2: *Frame 1 shows the global Ω as a function of flow-shear γ_E. Subsequent frames show the evolution of IM into GM for indicated values of flow-shears.*

The IM is obtained for a quadratic ITG drive profile $\eta_s = \eta_g(1.0 - \eta_c x^2)$, with $\eta_g = 2.0$, $\eta_c = 62.5$ and flow-shear $\gamma_E = 0$. As we gradually increase $|\gamma_E|$, the peak in the real part of the local complex mode frequency $\omega_0(x)$ is shifted relative to $\gamma_0(x)$, and $d\Omega_0(x)/dx \neq 0$. The IM is then seen to smoothly evolve into the GM (Fig. 2), as also observed in [4, 5]. These results have been benchmarked against the eigenmode solution to eqn. 1 developed in [4] to within 0.1%.

Time for eigenmode formation

Starting with arbitrary initial conditions, the IM forms over $\mathcal{O}(10^2)$ and the GM structure forms over $\mathcal{O}(10^3)$ growth-times γT_{eig}. These numbers suggest that non-linear regimes are likely to be entered before the linear mode structures are established. However, eqn. 1 is only valid for strongly unstable modes ($\eta_s \gg 1$).

If we increase η_s by 100%, we find that the global growth rate has increased by $\sim 80\%$, whereas T_{eig} only changes by 0.1%. Therefore close to marginal stability, it is possible that $\gamma T_{eig} \sim \mathscr{O}(1)$, and the structure and growth-rate of these linear modes may be important in determining non-linear transport. This should be investigated rigorously in the future using a more accurate plasma model.

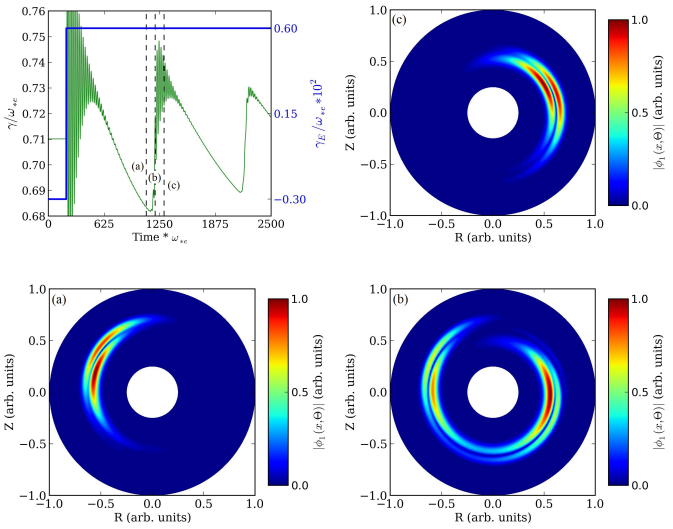

Figure 3: *Dashed vertical lines in frame 1 correspond to potential plots in subsequent frames (anti-clockwise).*

Floquet Modes

For plasma profiles held at high values of flow-shear ($\gamma_E \geq |0.4|$), we find that the linear mode rotates poloidally. It precesses rapidly through the bottom-half of the poloidal plane, slowing down in the top-half, performing many cycles, before eventually settling down at the top as a General Mode, with $\gamma_{FM}(t) \rightarrow \gamma_{GM}$ (Fig. 3). This is consistent with [6] which concludes that the Floquet form is generally a transient associated with starting conditions.

Dynamic plasma profiles

For results in this section, the flow-shear evolves over three time-scales, with all other plasma profiles held fixed.

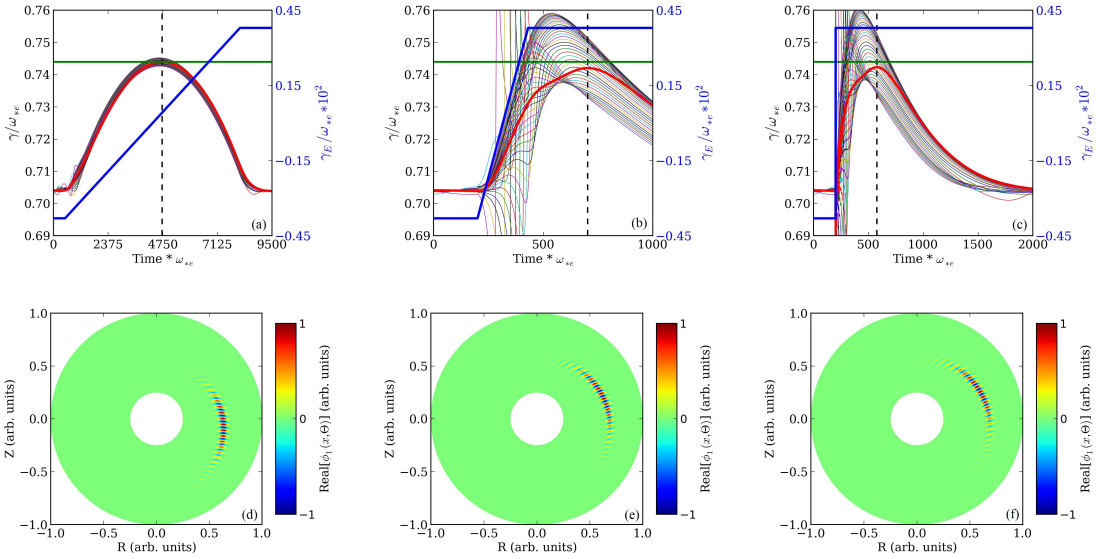

Figure 4: *Fig. 4a-4c show the evolution of the instability's global growth γ (red) as a function of flow-shear γ_E (blue). Fig. 4d-4f show the mode structure for the times indicated by the dashed-vertical lines in the frames above. The green-horizontal line indicates the IM growth-rate.*

Eigenmode time-scale For slowly varying profiles, the instability retains its eigenmode structure as it responds to the evolving flow (note that every γ_m has the same value at each time - Fig. 4a). Assuming typical $\omega_{*e} = 10^5\ s^{-1}$, the flow-shear evolves over ~ 100 ms time-scale.

Small-ELM relevant time-scale When profiles evolve over an $\mathcal{O}(1)$ ms time-scale, the eigenmode identity is lost. This is apparent since different Fourier harmonics grow at different rates (Fig. 4b). Nonetheless, $\gamma_{max} \sim \gamma_{\mathrm{IM}}$. However this γ_{max} is realised ~ 3 ms after the critical $\gamma_E = 0$ is passed (which would give the IM for flows held in time). Note this period is approximately the time it takes for the IM to form out of arbitrary initial conditions. Finally, we observe that the mode sits away from the outboard midplane at the time when $\gamma = \gamma_{max}$ (Fig. 4e).

Instantaneous profile reversal Starting with a mode sitting at the bottom of the poloidal plane, if the flow profile is immediately reversed such that the mode must balloon at the top, the instability again responds with a characteristic time, comparable to the time taken for the GM to form from initial noise. Further, all features identified for the small-ELM relevant ramp are recovered, and we additionally confirm that, independent of how rapidly the profiles change, the mode structure retains a *coherent* form as it gets convected poloidally (Fig. 4f).

Discussion

Could then a GM-IM transition provide a burst of instability corresponding to a small-ELM? A number of issues need to be addressed before a conclusion can be drawn. First, for our fluid model, a high growth implies that non-linear regimes are likely to be entered much before the linear mode structure could respond during a GM-IM transition. It is important that we compare the GM-IM transition time to growth-times close to a more realistic, marginally-stable, GM stability boundary. Secondly, if a GM-IM transition does indeed provide a burst in transport, the profiles are likely to reset and the GM must form again before driving another crash in the next small-ELM cycle. For our ITG model parameters and typical values of ω_{*e}, the GM formation time is significantly greater than the inter-small-ELM period ($\sim$ by a factor 10). Again one needs to ascertain this with a more realistic model of the pedestal, including kinetic ballooning mode physics, for example.

References

[1] J W Connor, J B Taylor and H R Wilson, *Phys. Rev. Lett.* **70** (1993) 1803

[2] J B Taylor, J W Connor and H R Wilson, *Plasma Phys. Control. Fusion* **38** (1996) 243

[3] J W Connor and J B Taylor, *Phys. Fluids* **30** (1987) 3180

[4] D Dickinson, C M Roach, J M Skipp and H R Wilson, *Physics of Plasmas* **21** (2014) 010702

[5] P A Abdoul, D Dickinson, C M Roach and H R Wilson, *Plasma Phys. Control. Fusion* **57** (2015) 065004

[6] J B Taylor and H R Wilson, *Plasma Phys. Control. Fusion* **38** (1996) 1999